REPUBLIC OF TÜRKİYE
ADANA ALPARSLAN TÜRKEŞ SCIENCE AND TECHNOLOGY UNIVERSITY

GRADUATE SCHOOL
MATERIALS ENGINEERING DEPARTMENT

PRODUCTION OF MULTIFUNCTIONAL NANOPARTICLE-REINFORCED POLYMER COMPOSITE SURFACES BY PHOTOPOLYMERIZATION METHOD AND INVESTIGATION OF PERFORMANCE CHARACTERISTICS

NADİYE MERVE AYDIN

M.Sc.

ADANA 2025

REPUBLIC OF TÜRKİYE
ADANA ALPARSLAN TÜRKEŞ SCIENCE AND TECHNOLOGY UNIVERSITY

GRADUATE SCHOOL
MATERIALS ENGINEERING DEPARTMENT

PRODUCTION OF MULTIFUNCTIONAL NANOPARTICLE-REINFORCED POLYMER COMPOSITE SURFACES BY PHOTOPOLYMERIZATION METHOD AND INVESTIGATION OF PERFORMANCE CHARACTERISTICS

NADİYE MERVE AYDIN

M.Sc.

THESIS ADVISOR
ASSOC. PROF. DR. İLKAN ÖZKAN

ADANA, 2025

CERTIFICATION OF APPROVAL

PRODUCTION OF MULTIFUNCTIONAL NANOPARTICLE-REINFORCED POLYMER COMPOSITE SURFACES BY PHOTOPOLYMERIZATION METHOD AND INVESTIGATION OF PERFORMANCE CHARACTERISTICS

This **M.Sc.** thesis, **completed under the conditions determined by the relevant regulations**, by **NADİYE MERVE AYDIN with student number** 22800801002 in **Adana Alparslan Türkeş Science and Technology University Institute of Graduate School** Materials Engineering **Department**, has been evaluated by the following academic committee, and approved in accordance with the relevant articles of the "Adana Alparslan Türkeş Science and Technology University Graduate Education Regulations".

Prof. Dr. Mustafa AKYOL

Institute of Graduate School Manager

Assoc. Prof. Dr. İlkan ÖZKAN

Head of the Department

Assoc. Prof. Dr. İlkan ÖZKAN

Academic Adivisor

Thesis Advisory Committee Members

Academic Title, Name Surname

Adana Alparslan Türkeş Science and Technology University

Assoc. Prof. Dr. İlkan ÖZKAN

Adana Alparslan Türkeş Science and Technology University

Prof. Dr. Mustafa GÜNEŞ

Adana Alparslan Türkeş Science and Technology University

Prof. Dr. Pınar DURU BAYKAL

Çukurova University

Thesis Defence Date

26/08/2025

DECLARATION OF CONFORMITY

In this thesis study, which was prepared following the thesis writing rules of Adana Alparslan Türkeş Science and Technology University Institute of Graduate School, I declare that I provide all the information, documents, evaluations and results in accordance with scientific ethics and moral codes without resorting to any means or assistance that would be contrary to scientific ethics and traditions. I also declare that I refer to all of the articles I used in this study with appropriate references and accept all moral and legal consequences if a situation is found contrary to my statement regarding my work.

26/08/2025

[Signature]

Nadiye Merve AYDIN

ÖZET

Fotopolimerizasyon Yöntemiyle Nanopartikül Takviyeli Multifonksiyonel Polimer Kompozit Yüzeylerin Üretimi ve Performans Özelliklerinin Araştırılması

Nadiye Merve AYDIN

Yüksek Lisans, Malzeme MühendisliğiAnabilim Dalı

Danışman: Doç. Dr. İlkan ÖZKAN

Ağustos 2025, 49 sayfa

Son yıllarda, stereolitografi (SLA) tipi üç boyutlu (3B) yazıcılar, kompozit malzemelerin üretiminde yüksek hassasiyet, düşük yüzey pürüzlülüğü ve atık minimizasyonu gibi avantajları nedeniyle giderek önem kazanmıştır. Eklemeli üretim (EÜ) olarak da bilinen 3B baskı, geleneksel üretim yöntemleriyle imkânsız ya da zor olan karmaşık geometrilere sahip tasarımların kolaylıkla üretilmesine olanak sağlamaktadır. Bu teknolojinin sunduğu geniş tasarım esnekliği ve üretim süreçlerindeki verimlilik, biyomedikal, otomotiv, havacılık ve savunma gibi çeşitli sektörlerde yoğun olarak kullanılmasını sağlamıştır [1,2].

İlk kez 1980'li yıllarda UV lazerler kullanılarak tanıtılan SLA teknolojisi, sıvı fotopolimer reçinelerin bilgisayar kontrollü ultraviyole ışınlarıyla katman katman işlenerek katılaştırılması prensibine dayanmaktadır. Bu süreçte yarı sıvı hammaddeler, yüksek çözünürlükte ve hassas geometrilerle katı forma dönüştürülür. SLA tipi 3B baskı sistemleriyle üretilen parçaların mekanik, termal ve elektriksel gibi fonksiyonel özellikleri, geleneksel üretim yöntemleriyle karşılaştırıldığında daha kontrollü bir şekilde optimize edilebilmektedir. Son dönemde teknolojideki gelişmelerle birlikte, SLA ile nanokompozit malzeme üretimine yönelik araştırmalar önemli ölçüde artmıştır. SLA teknolojisinin sunduğu tasarım özgürlüğü, üretim hızı ve maliyet etkinliği, bu alandaki araştırmalara önemli bir ivme kazandırmıştır.

Bu projede, fotopolimer reçine içerisine %1, %3 ve %5 oranlarında nanopartiküller katılarak nanokompozit yüzeyler üretilmiştir. Numuneler SLA tipi Anycubic marka yazıcı kullanılarak, her bir katmanın kalınlığı 50 mikron olacak şekilde katman katman basılmıştır. Üretilen numunelerin yüzey özdirenç özellikleri TS EN 1149-1:2006 standardına göre, 25°C sıcaklık ve %50 bağıl nem koşullarında ELME Multimeg cihazıyla ölçülmüştür. Yapılan ölçümler sonucunda tüm numunelerin yüzey özdirenç değerlerinin 10^{12} ohm'dan yüksek olduğu belirlenmiştir. Bu değerler, numunelerin yüksek elektriksel yalıtkanlık özelliğine sahip

olduğunu göstermektedir. Ayrıca, antibakteriyel aktivite testleri TS ISO 22196 standardına göre gerçekleştirilmiş olup, nanokompozitlerin tüm katkılama oranlarında S. aureus ve E. coli bakterilerine karşı %99'un üzerinde etkinlik gösterdiği tespit edilmiştir. Elektromanyetik kalkanlama etkinliği ise saçılım parametreleri üzerinden hesaplanarak değerlendirilmiş ve 8-12 GHz frekans aralığında 5 dB'den düşük kalkanlama etkinliği gösterdiği belirlenmiştir. Böylelikle üretilen nanokompozitlerin elektriksel yalıtım, antibakteriyel uygulamalar ve elektromanyetik dalgalara karşı geçirgen yapıları ile çeşitli uygulama alanlarında kullanılabileceği ortaya konulmuştur.
Anahtar Kelimeler: SLA reçine, 3B yazıcı, fotopolimer, eklemeli üretim, kompozit malzeme

ABSTRACT

Production of Multifunctional Nanoparticle-Reinforced Polymer Composite Surfaces by Photopolymerization Method and Investigation of Performance Characteristics

Nadiye Merve AYDIN
M.Sc., Department of Materials Engineering

Supervisor: Assoc. Prof. Dr. İlkan ÖZKAN

August 2025, 49 pages

In the recent years, Stereolithography (SLA) type three-dimensional (3D) printers have gained increasing importance in the production of composite materials due to their high precision, low surface roughness, and minimal material waste. Also known as additive manufacturing (AM), 3D printing enables the fabrication of complex geometries that are difficult or impossible to achieve with conventional manufacturing techniques. This technology offers design flexibility and production efficiency, making it widely used in biomedical, automotive, aerospace, and defense sectors [1,2].

SLA technology, first introduced in the 1980s using UV lasers, is based on the principle of layer-by-layer polymerization of liquid photopolymer resins via computer-controlled ultraviolet light. During the process, semi-liquid raw materials are solidified into high-resolution and dimensionally accurate geometries. The mechanical, thermal, and electrical properties of parts produced using SLA can be precisely optimized compared to conventional production methods. With recent technological advancements, research on the fabrication of nanocomposite materials via SLA has significantly increased. The design freedom, cost-effectiveness, and production speed offered by SLA technology have accelerated investigations in this field.

In this thesis, nanocomposite surfaces were fabricated by incorporating nanoparticles into a photopolymer resin with concentrations of 1%, 3%, and 5%. The specimens were produced layer-by-layer using an Anycubic SLA printer with a layer thickness of 50 microns. Surface resistivity measurements were performed in accordance with the TS EN 1149-1:2006 using an ELME Multimeg device under controlled conditions of 25°C and 50% relative humidity. The results indicated that all samples exhibited surface resistivity values exceeding 10^{12} ohms, confirming their high electrical insulation performance. Additionally, antibacterial activity tests, conducted in accordance with TS ISO 22196, revealed that all formulations exhibited more than 99% effectiveness against *S. aureus* and *E. coli*. Electromagnetic shielding effectiveness (EMSE) was evaluated based on scattering parameters, and the materials demonstrated a shielding effectiveness of less than 5 dB in the 8–12 GHz frequency range. Consequently, the developed nanocomposites show potential for use in applications requiring electrical insulation, antimicrobial surfaces, and partial permeability to electromagnetic waves.

Keywords : SLA resin, 3D printer, photopolymer, additive manufacturing, composite materials

Dedication

I dedicate this thesis to my beloved family, whose unwavering support, love, and encouragement have been my greatest strength throughout this journey. Without their constant belief in me, this achievement would not have been possible.

I would also like to express my heartfelt gratitude to my teachers, whose wisdom, guidance, and patience have shaped my path. Their dedication to my education has been instrumental in reaching this milestone.

ACKNOWLEDGEMENTS

I would like to express my gratitude to my advisor Assoc. Prof. Dr. İlkan ÖZKAN who is the head of the Materials Science and Engineering Department at Faculty of Engineering, for his support, guidance, and extensive expertise throughout my master's degree.

Finally, I want to thank my family from the bottom of my heart. Their steadfast moral and financial support has been essential to my academic career and all of my choices.

This work was supported by Adana Alparslan Türkeş Science and Technology University Scientific Research Coordination Unit. Project Number: 24303001

Nadiye Merve AYDIN

Adana, 2025

TABLE OF CONTENTS

LIST OF FIGURES

LIST OF TABLES

LIST OF ABBREVIATIONS

Si	: Silicon
Ag	: Silver
Cu	: Copper
Ti	: Titanium
TiO2	: Titanium dioxide
CuO	: Copper oxide
UV	: Ultraviolet
IR	: Infrared
SLA	: Stereolithography
SLS	: Selective Laser Sintering
LOM	: Laminated Object Manufacturing
3DP	: Three-Dimensional Printing
CAD	: Computer-aided Design
NRPC	: Nanoparticle Reinforced Polymer Composite
AM	: Added Manufacturing
GO	: Graphene Oxide
CNT	: Carbon Nanotube
FDM	: Fused Deposition Modeling
PLA	: Polylactic Acid
FFF	: Fused Filament Fabrication
ABS	: Acrylonitrile Butadiene Styrene

LIST OF SYMBOLS

Ω **:** Ohm unit

dB **:** Decibel

GHz **:** Gigahertz

1. INTRODUCTION

In recent years, composite material production has come to the forefront with stereolithography (SLA) type three-dimensional (3D) printers due to their high processability and low surface defects. Also known as additive manufacturing (AM), 3D printing can be used to create formats with complex geometries. In these systems, which have very wide design and flexible production possibilities, metallic, polymer and composite parts can be produced with very little waste [1,2]. Among the applications of this processing technology are process-specific parts produced in biomedical, automotive, maintenance, etc. sectors [3]. 3D printing was first introduced in the early 1980s via the stereolithography process and UV lasers were used to reproduce polymer layers in 3D [4]. In the working system of SLA technology, fluid photopolymer resins are processed in 3D printers and converted into solid form. In the production process, the use of semi-fluid raw materials can be used in a designed entire structure by creating layers with computer-controlled ultraviolet rays. For each layer, the process is repeated step by step and a 3D solid model version is included at the end of the printing. With the rapid start of the processes, it is possible to obtain detailed and clean prints in this production method.

With the technological advances, it is indicated that research on the use of 3D printers in the field of composite material production continues to increase significantly. The potential to overcome the limitations of traditional production methods, the design freedom and personalization ability offered by 3D printers have accelerated research in this field. The importance of this research becomes even more evident when the critical role of composite materials in a wide range of applications is brought to the fore. In sectors where there is a high demand for lightweight and high-strength materials, such as the aircraft and automotive industries, it is seen that more efficient and optimized parts can be produced with the manufacturable use of 3D printers. This can provide great advantages both in factors such as fuel economy and cost savings. At the same time, 3D printers aim to offer the potential to better adapt to individual needs and provide personalized solutions in areas such as medical implants, prostheses and sports products for composite material production. This brings with it the enhancing effects on human life.

In this context, the increasing research in the field of composite material production of 3D printers will provide the potential for changes in industrial production. High statistical, privately stored and sustainable data are emerging, showing that research in this field is of great importance not only in academic terms, but also in industrial and social terms.

Gardner et al. conducted a study exploring the suitability of carbon nanotube (CNT) filaments as raw materials for additive manufacturing. They addressed the challenges of using the material in fused deposition modeling (FDM) type production systems and the potential to produce multifunctional components. They examined the mechanical and electrical properties of the samples they produced and demonstrated the potential to produce multifunctional components by manufacturing a quadcopter frame using the relevant method. CNT reinforcement added electrical conductivity to the samples, indicating the potential of using CNT in FDM-type production [5].

Gkartzou et al. researched the use of a sustainable material made from lignin and polylactic acid (PLA) blend for 3D printing. They examined the physical, mechanical, and thermal properties of different PLA/lignin blends and aimed to identify the best composition for 3D printing filament production. They investigated the effects of extrusion temperature, printing speed, and filament diameter parameters on the morphology of the samples. The study concluded that extrusion temperature and printing speed significantly impacted the morphology of printed objects. Researchers emphasized lignin's potential as an alternative material to petroleum-derived plastics in the growing 3D printing market [6].

Podsiadły et al. explained the production process of nanocomposite filaments based on carbon nanotubes (CNT) and acrylonitrile butadiene styrene (ABS) polymer for FDM additive manufacturing. They extensively examined the mechanical and electrical properties of the samples they produced. They showed that the CNT content significantly affected the mechanical properties and electrical conductivity of printed samples. They emphasized that ABS/CNT composites could be promising functional materials for FDM-type production, especially for structural and electronic components and sensors [7].

Fico et al. discussed the challenges encountered in turning prototypes produced by Fused Filament Fabrication (FFF) into functional objects for industrial applications due to the low and anisotropic mechanical properties of polymer components produced by the FFF method.

They highlighted the limitations of FFF-type production, such as low surface quality, low production speed, and limited material options. They stressed the importance of sustainable material selection for reducing environmental impacts and making this technology a sustainable production method [8].

Mussadiq et al. investigated the impact of graphene oxide (GO) distribution on the mechanical and thermal properties of 3D printed nanocomposites. Using the Stereolithography (SLA) technique, they attempted to optimize the dispersion of GO nanoparticles within a polymer matrix. They found that nanoparticle distribution had a significant impact on mechanical properties and highlighted its potential in functional applications. They aimed to develop a nanocomposite resin with well-dispersed nanoparticles for polymer-based 3D printing [9].

Aumnate et al. explored the production of ABS/graphene oxide composite filaments for 3D printing applications. They aimed to improve ABS's mechanical, thermal, and electrical properties by adding graphene oxide fillers. They discussed the methods for distributing graphene oxide in the ABS matrix and evaluated the processability of ABS/GO composites regarding thermal and rheological properties. They 3D printed a model using ABS/GO composite filament with ultrasonic mixing. They emphasized that the addition of GO improved tensile strength and electrical conductivity [10].

Ely et al. examined the physical and chemical properties of 3D-printed layers loaded with copper-nickel nanotubes. They used layer-by-layer photopolymerization to incorporate nanotubes into a new resin and characterized the morphological, mechanical, thermal, and chemical properties of pure and nanotube-loaded resins. They focused on optimizing the distribution of nanotubes within the composite resin, highlighting the potential for enhancing electromechanical properties and suggesting future research directions for developing composite materials [11].

Aktitiz et al. investigated the applications of 3D printing technology in various industries, including automotive, biomedical, and energy. They discussed the most common additive manufacturing methods, such as Stereolithography (SLA), Fused Deposition Modeling

(FDM), Selective Laser Sintering (SLS), Laminated Object Manufacturing (LOM), Three-Dimensional Printing (3DP), and Laser Metal Deposition. They emphasized the importance of developing polymer matrix composites (PMCs) with variable compositions, sizes, and types of reinforcement and matrix structures. They discussed the potential applications of 3D-printed composite structures in different industries and highlighted the need for further research in this field [12].

Chiulan et al. focused on using stereolithography (SLA) to create photopolymerizable graphene-based resins to develop polymer matrix composites (PMCs), with a particular emphasis on medical applications. They discussed SLA-produced objects' mechanical properties and biocompatibility and their potential use in biosensors and medical implants. They suggested that integrating graphene into polymer matrices could develop composites with enhanced mechanical properties for applications in various fields, including tissue engineering and organ development. However, they highlighted the need for further research to address challenges related to material availability, biocompatibility, printing speed, and resolution [13].

Vinita et al. researched using a self-healing microcapsule catalyst system to enhance the mechanical strength and lifespan of 3D-printed objects using stereolithography (SLA)-based 3D printing. They synthesized microcapsules filled with healing liquids and examined their distribution within composite materials. They discussed the potential of such microcapsules to extend life and improve the sustainability of SLA 3D-printed materials, emphasizing the need for further research to optimize their effectiveness [14].

Balwant et al. investigated the role of 3D printing in producing customized products with complex designs using various materials, including polymers, metals, ceramics, and composites. They explored the development of in-house Polymer Matrix Composites (PMCs) with variable compositions, sizes, and types of reinforcement and matrix structures. They highlighted the advantages of 3D printing in terms of rapid prototyping and cost-effective customization of products. They discussed its applications in various industries, including biomedical, aerospace, military, automotive, and jewelry. They underscored the importance of ongoing research in 3D printing and material development [15,16].

Figure 1. 1. The SLA 3D printer used in the research (*Anycubic Photon M3 Max*, n.d.) [17].

Eren and his colleagues investigated the mechanical and electrical properties of photopolymer nanocomposite materials reinforced with carbon-based nanoparticles produced by DLP. Nanocomposites were produced by incorporating varying proportions of Multi Walled Carbon Nanotubes (MWCNT), reduced Graphene Oxide (rGO) and combinations of Carbon Black and Carbon Nanotubes (CB/CNT) into the photopolymer matrix. This study is the first to investigate the most effective concentrations of three different carbon-based nanoparticles and the effect of their homogeneous distribution on the performance of the composites with a holistic approach. Morphological analysis of the composites using optical microscopy and Scanning Electron Microscopy (SEM) revealed that the nanoparticle distribution plays a critical role in determining the composite properties. The findings showed that the incorporation of nanoparticles at low proportions (up to 0.5 wt%) led to a significant improvement in the ultimate tensile strength of the photopolymer, with an increase of up to 82% [18].

Qiu et al. developed UV-curable nanocomposite coatings by integrating functionalized phosphazene-containing nanotubes into a polyurethane acrylate matrix. The coatings showed improved thermal stability and mechanical strength due to the covalent bonding between the nanotubes and the polymer matrix. This study developed UV-curable nanocomposite coatings by incorporating acryloyl-functionalized phosphazene nanotubes (f-PZS) into a polyurethane acrylate (PUA) matrix. The functionalized nanotubes were synthesized using a mild in situ method and the thermal and mechanical properties of the coating were improved. The best performance was observed at 3.0 wt% f-PZS with an increase in thermal stability of 36.3°C at 1.0 wt%. The improvements were concluded to be due to the improved interfacial bonding resulting from the covalent functionalization [19].

Ingrosso et al. developed a UV-curable nanocomposite by incorporating surface-modified TiO_2 nanocrystals into methacrylic-siloxane resin. It was observed that the addition of TiO_2 improved both the photopolymerization efficiency and the mechanical properties of the material due to better dispersion and interaction with the resin [20].

Abatay et al. focused on creating antibacterial composite stone materials by incorporating inorganic agents such as silver, zinc oxide, calcium oxide, titanium oxide, and magnesium oxide. These composite stones, mainly consisting of 90% quartz aggregate and 10% thermoset polyester resin, were processed using vibropress techniques. In their study, they evaluated the mechanical, thermal, and morphological properties of these materials and evaluated their antibacterial activity against Escherichia coli and Bacillus subtilis using the colony count method. They noted that the samples containing silver in particular showed the highest antibacterial activity with a reduction of approximately 99% in bacterial colonies [21].

Amrhar et. al. ın this review article, they have investigated a comprehensive overview of polymeric nanocomposite coatings designed for antimicrobial and antiviral applications. They have highlighted how nanomaterials such as metal and metal oxide nanoparticles enhance the antimicrobial activity of polymer coatings through mechanisms such as disrupting microbial membranes or releasing active agents.The integration of various nanomaterials, such as metal and metal oxide nanoparticles, into polymer matrices to enhance their protective functions is discussed. The article also discusses current applications in healthcare and packaging and outlines challenges such as nanoparticle distribution parameters and long-term stability [22].

Díez-Pascual et. al. ın this comprehensive review, they investigated the development of polymer nanocomposites enriched with graphene-based materials such as graphene oxide (GO) and reduced graphene oxide (rGO), focusing on their antibacterial properties. The authors categorized these nanocomposites based on the type of polymer matrix used: acrylic and methacrylic polymers, biodegradable synthetic polymers, and natural polymers. The review investigated the mechanisms by which graphene and its derivatives exert antimicrobial effects, including physical disruption of bacterial membranes, induction of oxidative stress, and capture of microorganisms. Additionally, the paper discussed the potential applications of these nanocomposites in various areas, such as medical devices, food packaging, and water treatment systems [23]. The authors concluded that with further research, graphene-polymer nanocomposites could become effective, safe, and scalable antimicrobial agents.

- **Graphene-based Materials**: The article primarily focuses on graphene oxide (GO), reduced graphene oxide (rGO), and other graphene derivatives. These materials are incorporated into polymer matrices to form nanocomposites with enhanced antibacterial effects.
- **Polymer Matrices**: The review categorizes polymer nanocomposites based on the type of polymer used. These include:

- **Acrylic and Methacrylic Polymers**: Widely used due to their versatility and ease of processing.
- **Biodegradable Synthetic Polymers**: Such as polylactic acid (PLA), which offer environmentally friendly alternatives.
- **Natural Polymers**: Including chitosan, which are biocompatible and sustainable.

- **Antibacterial Mechanisms**: The article describes several mechanisms through which graphene-based materials exhibit antibacterial activity:

- **Physical Disruption**: Graphene and its derivatives physically disrupt the bacterial cell membrane, leading to cell death.
- **Oxidative Stress**: The materials generate reactive oxygen species (ROS) that induce oxidative damage to bacteria.
- **Electrostatic Interactions**: The negative charge on graphene oxide facilitates strong interactions with the positively charged bacterial cell wall.
- **Nanoscale Effects**: The small size of graphene derivatives allows them to penetrate bacterial cells and disrupt intracellular functions.

- **Applications**:

- **Medical Devices**: The incorporation of graphene-based nanocomposites into medical devices, such as wound dressings and implants, can prevent bacterial infections and enhance the longevity of devices.
- **Food Packaging**: Graphene-based nanocomposites can be used in food packaging to

provide antimicrobial properties, thus extending the shelf life of food products.

- **Water Purification**: Graphene materials also show promise in water treatment, where they can help remove pathogens from contaminated water [23].

Olmos et. al. focused on materials enriched with inorganic nanoparticles (e.g. Ag, Cu, TiO_2, ZnO), surface nanostructuring, and antifouling strategies. Key findings included bacterial inhibition mechanisms such as membrane disruption and reactive oxygen species (ROS) production.In the paper, they investigated how adding inorganic particles such as silver (Ag), copper (Cu), zinc oxide (ZnO), and titanium dioxide (TiO_2) to polymers significantly increased their antibacterial functionality. These particles were found to act through mechanisms such as disrupting bacterial membranes or generating reactive oxygen species (ROS) [24].

Avila et al. (2020) investigated the reinforcement of SLA 3D-printed polymer resins using anatase-phase TiO_2 nanoparticles annealed at temperatures from 400 °C to 1000 °C. The study showed that nanoparticles annealed at 800 °C provided optimal mechanical improvements, including a 103% increase in tensile strength and 32% enhancement in elastic modulus compared to unfilled resins. These improvements were linked to enhanced nanoparticle dispersion and stronger interfacial bonding within the polymer matrix. The study showed that incorporating low concentrations of TiO_2 nanoparticles into photopolymer resins can significantly enhance the mechanical and thermal properties of 3D printed composites without compromising printability. The optimum concentration of 0.4 wt% TiO_2 was determined and was found to balance improved compressive strength and toughness with minimal adverse effects on tensile properties and print quality. Higher concentrations were observed to cause nanoparticle aggregation, adversely affecting mechanical performance and surface quality. These findings demonstrate that carefully controlled incorporation of TiO_2 NPs can produce strong, lightweight, and thermally stable polymer nanocomposites suitable for applications in the aerospace, automotive, and biomedical fields. [25].

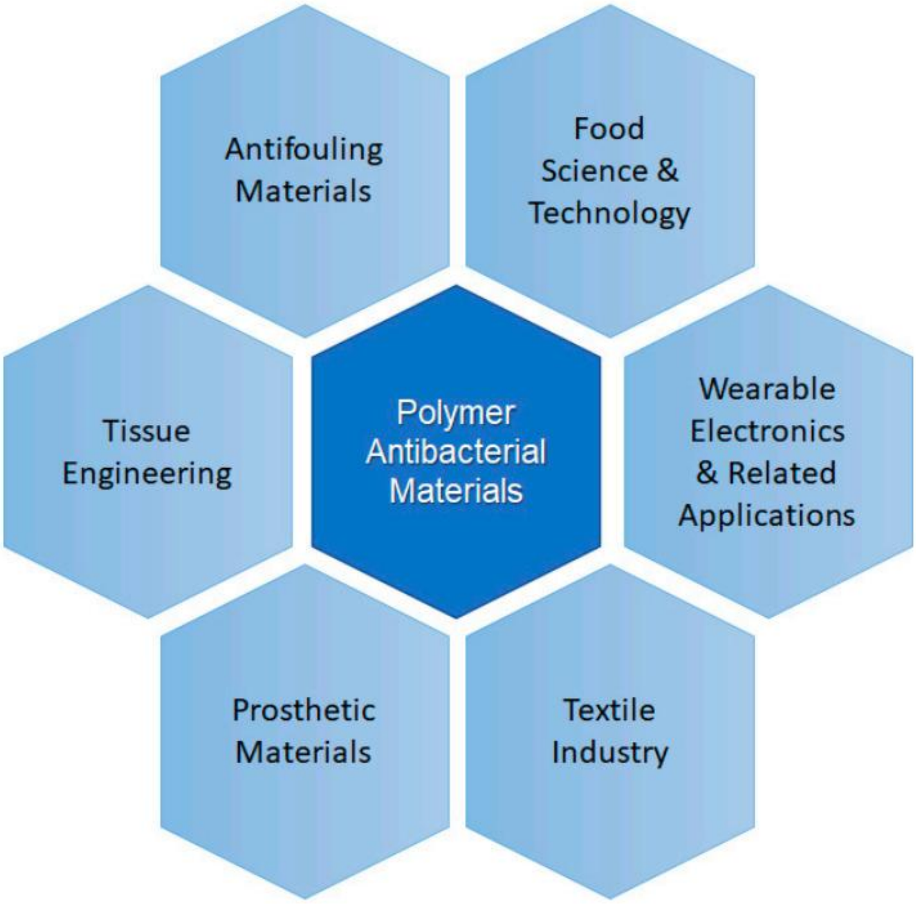

Figure 1. 2. Various application areas for polymer-based antibacterial materials [24].

Gil, Monteiro, and Colorado (2024) investigated the fabrication of polymer matrix nanocomposites by incorporating copper nanoparticles (Cu-NPs) into a UV-curable photopolymer resin using tub photopolymerization (VPP) additive manufacturing. Cu-NP concentrations of 0.0, 0.5, and 1.0 wt% were used in the study. Mixing was performed by a combination of vortex and ultrasonic methods to ensure effective dispersion. Post-curing with UV light improved the mechanical properties of the printed samples. Scanning electron microscopy (SEM) confirmed uniform nanoparticle distribution, while tensile testing revealed that UV irradiation improved tensile strength, but higher nanoparticle loadings led to increased viscosity and potential agglomeration that could affect mechanical performance. The research highlights the potential of this low-cost and accessible method to fabricate nanocomposites in electronic, structural components, and biomedical applications [26].

2. THEORETICAL FOUNDATIONS AND LITERATURE REVIEW

Gkartzou et al. researched the use of a sustainable material made from lignin and polylactic acid (PLA) blend for 3D printing. They examined the physical, mechanical, and thermal properties of different PLA/lignin blends and aimed to identify the best composition for 3D printing filament production. They investigated the effects of extrusion temperature, printing speed, and filament diameter parameters on the morphology of the samples. The study concluded that extrusion temperature and printing speed significantly impacted the morphology of printed objects. Researchers emphasized lignin's potential as an alternative material to petroleum-derived plastics in the growing 3D printing market [6].

Podsiadły et al. explained the production process of nanocomposite filaments based on carbon nanotubes (CNT) and acrylonitrile butadiene styrene (ABS) polymer for FDM additive manufacturing. They extensively examined the mechanical and electrical properties of the samples they produced. They showed that the CNT content significantly affected the mechanical properties and electrical conductivity of printed samples. They emphasized that ABS/CNT composites could be promising functional materials for FDM-type production, especially for structural and electronic components and sensors [7].

Fico et al. discussed the challenges encountered in turning prototypes produced by Fused Filament Fabrication (FFF) into functional objects for industrial applications due to the low and anisotropic mechanical properties of polymer components produced by the FFF method. They highlighted the limitations of FFF-type production, such as low surface quality, low production speed, and limited material options. They stressed the importance of sustainable material selection for reducing environmental impacts and making this technology a sustainable production method [8].

Mussadiq et al. investigated the impact of graphene oxide (GO) distribution on the mechanical and thermal properties of 3D printed nanocomposites. Using the Stereolithography (SLA) technique, they attempted to optimize the dispersion of GO nanoparticles within a polymer matrix. They found that nanoparticle distribution had a significant impact on mechanical properties and highlighted its potential in functional applications. They aimed to develop a nanocomposite resin with well-dispersed nanoparticles for polymer-based 3D printing [10].

Aumnate et al. explored the production of ABS/graphene oxide composite filaments for 3D printing applications. They aimed to improve ABS's mechanical, thermal, and electrical properties by adding graphene oxide fillers. They discussed the methods for distributing graphene oxide in the ABS matrix and evaluated the processability of ABS/GO composites regarding thermal and rheological properties. They 3D printed a model using ABS/GO composite filament with ultrasonic mixing. They emphasized that the addition of GO improved tensile strength and electrical conductivity [10].

Ely et al. examined the physical and chemical properties of 3D-printed layers loaded with copper-nickel nanotubes. They used layer-by-layer photopolymerization to incorporate nanotubes into a new resin and characterized the morphological, mechanical, thermal, and chemical properties of pure and nanotube-loaded resins. They focused on optimizing the distribution of nanotubes within the composite resin, highlighting the potential for enhancing electromechanical properties and suggesting future research directions for developing composite materials [11].

Aktitiz et al. investigated the applications of 3D printing technology in various industries, including automotive, biomedical, and energy. They discussed the most common additive manufacturing methods, such as Stereolithography (SLA), Fused Deposition Modeling (FDM), Selective Laser Sintering (SLS), Laminated Object Manufacturing (LOM), Three-Dimensional Printing (3DP), and Laser Metal Deposition. They emphasized the importance of developing polymer matrix composites (PMCs) with variable compositions, sizes, and types of reinforcement and matrix structures. They discussed the potential applications of 3D-printed composite structures in different industries and highlighted the need for further research in this field [12].

Chiulan et al. focused on using stereolithography (SLA) to create photopolymerizable graphene-based resins to develop polymer matrix composites (PMCs), with a particular emphasis on medical applications. They discussed SLA-produced objects' mechanical properties and biocompatibility and their potential use in biosensors and medical implants. They suggested that integrating graphene into polymer matrices could develop composites with enhanced mechanical properties for applications in various fields, including tissue engineering and organ development. However, they highlighted the need for further research to address challenges related to material availability, biocompatibility, printing speed, and resolution [13].

Vinita et al. researched using a self-healing microcapsule catalyst system to enhance the mechanical strength and lifespan of 3D-printed objects using stereolithography (SLA)-based 3D printing. They synthesized microcapsules filled with healing liquids and examined their distribution within composite materials. They discussed the potential of such microcapsules to extend life and improve the sustainability of SLA 3D-printed materials, emphasizing the need for further research to optimize their effectiveness [14].

Balwant et al. investigated the role of 3D printing in producing customized products with complex designs using various materials, including polymers, metals, ceramics, and composites. They explored the development of in-house Polymer Matrix Composites (PMCs) with variable compositions, sizes, and types of reinforcement and matrix structures. They highlighted the advantages of 3D printing in terms of rapid prototyping and cost-effective customization of products. They discussed its applications in various industries, including biomedical, aerospace, military, automotive, and jewelry. They underscored the importance of ongoing research in 3D printing and material development [15].

3.MATERIALS AND METHODS

3.1. MATERIALS

In this study, the matrix material was used the standard photopolymer resin produced by the commercial company named as Anycubic. This resin has a UV-curable system with a wavelength of 405 nm, low viscosity, and good flow properties. It was chosen due to its compatibility with SLA-type 3D printers, its ability to print high-resolution details, and its suitability for forming a homogeneous structure. The resin used is green in color and is particularly preferred for precision part production. Thanks to its photopolymeric nature, it demonstrates effective cross-linking during the layered manufacturing process, resulting in products with high mechanical strength. Images of the composite materials produced with 1%, 3%, and 5% reinforcement are presented in Figure 3.1.

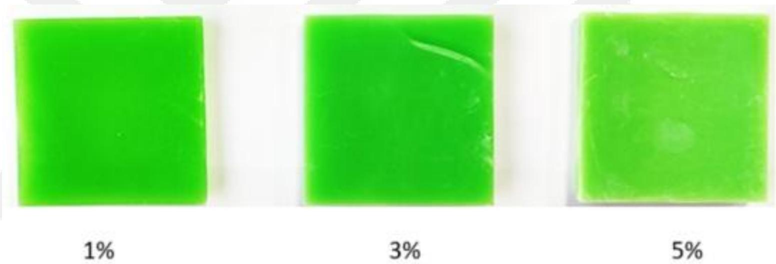

Figure 3. 1. The composite materials produced with 1%, 3%, and 5% reinforcement**.**

The properties of the used resin are provided in the table 1 below:

Table 3.1. Properties of the used resin

Property	Value
Viscosity (25 °C)	552 mPa·s
Tensile Strength	23.4 MPa
UV Curing Wavelength	405 nm
Liquid Density	1.100 g/cm^3
Solid Density	1.184 g/cm^3
Elongation at Break	14.2%
Hardness	Shore 79 D
Layer Thickness	50 microns
Layer Curing Time	5–15 seconds
Bottom Layer Curing Time	20–60 seconds
Softening Temperature	65–70 °C

The reinforcing phase used in the study was bismuth oxide (Bi_2O_3) nanoparticles with 99.99% purity. These nanoparticles are yellow in color, have an average particle size ranging from 75–195 nm, and exhibit a spherical morphology. The specific surface area is 4.0–6.0 m^2/g, the true density is 9.2 g/cm^3, the molecular weight is 466 g/mol, and the melting point is 810 °C. These properties make bismuth oxide a suitable additive for applications involving electrical insulation and electromagnetic wave transmission, due to its high atomic number and density. Furthermore, it was chosen for this study based on its widely reported antibacterial effectiveness in the literature. Its spherical morphology and narrow particle size distribution facilitate homogeneous dispersion within the resin, improving composite performance.

As a cleaning agent, 99% pure isopropyl alcohol (IPA) was used to remove any uncured resin left on the surface after production. This step ensured effective removal of surface residues and excess material, standardizing the specimens before testing. Following printing, the samples were washed in an isopropyl alcohol bath, allowed to dry to eliminate residual alcohol, and subjected to final UV curing.

3.2. METHOD

3.2.1. Stereolithography

Stereolithography (SLA) 3D printers are 3D printers that use resin as a material. Light from the laser light source in an SLA 3D printer cures the photosensitive resin poured into the printer's print chamber by bonding the resin's molecular chains together, creating a 3D model as the resin hardens.For prints that require a higher quality surface resolution and lack of layer imagery, production should be done with an SLA 3D printer [16]. Comparison of the different types of 3D printing technology given in Figure 3.2 and Parts of Anycubic Photon M3 Max SLA 3D Printer given in Figure 3.3.

	SLA	FDM	SLS	LOM	DLP
Applications	Excellent for form testing Best process for water resistant material	Suitable for prototypes Home use applications	Ideal for functional parts with various application Suitable for complex shape object Heat and chemical resistant	Ideal for nonfunctional prototypes	Similar to SLA
Overall Accuracy	Most accurate printing process	Accurate and reliable process	not very accurate	Slightly less dimensional accuracy	High Accuracy
Material Options	ABS Semi-flexible materials High temperature ABs	Thermoplastic materials	Nylon Glass-Filled Nylon	Paper Plastic Metal	Similar to SLA
Finish Options	Excellent surface finish	Standard Finish	Standard Finish	Wood like characteristics and can be treated similarly	Good finish High resolution
Post Processing Requirement	Requires post processing to remove support structure	Requires post processing to remove support structure	Does not require support structure, less post processing requires	Polishing Painting	Requires Post processing

Figure 3. 2. Comparison of the different types of 3D printing technology [27].

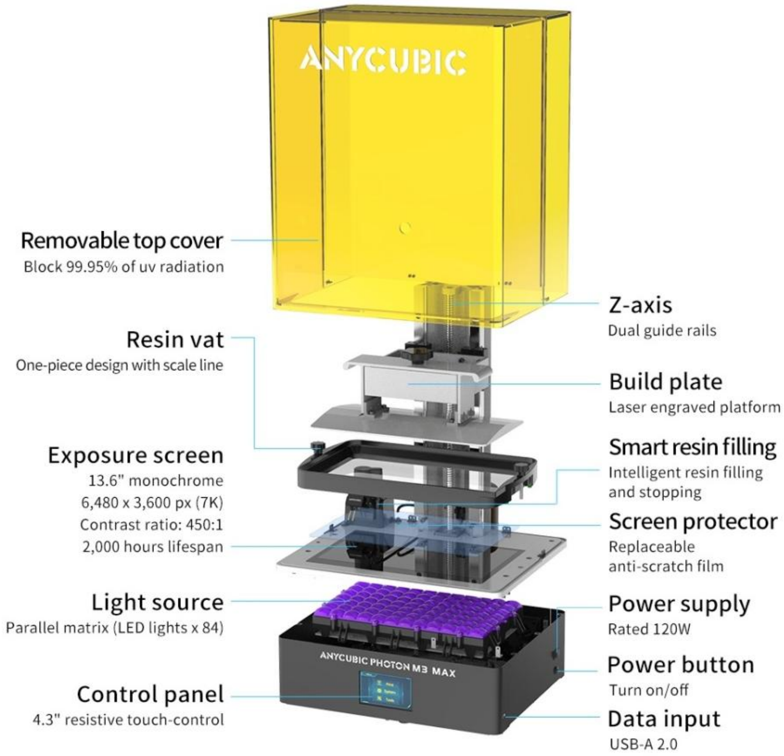

Figure 3. 3. Parts of Anycubic Photon M3 Max SLA 3D Printer [28].

On SLA 3D printers, before cleaning the support materials after printing, the removed model should be cleaned in an isopropyl alcohol bath. Any support materials should be removed and then exposed to UV light to harden and stabilize the model.Stereolithography is often used for ease of use when intricate details and/or a very smooth surface finish are crucial. It is a suitable method when the model's strength and durability are not crucial (resin models can be damaged by prolonged sun exposure) [16].

3.2.2 Characterization and Test Procedures

3.2.2.1 Scanning Electron Microscopy – Energy Dispersive X-ray Spectroscopy (SEM–EDS) Analyses

To thoroughly assess the surface morphology and chemical composition of the produced nanocomposites, Scanning Electron Microscopy (SEM) and Energy Dispersive X-ray Spectroscopy (EDS) analyses were conducted at the Central Laboratory of Çukurova University using a FEI Quanta 650 Field Emission SEM. Due to the insulating nature of Bi_2O_3 and the resin, a thin conductive coating of gold-palladium (60/40%) was applied to the specimen surfaces prior to analysis using a Quorum Q150RS sputter coater under an argon atmosphere, with a thickness of 5–10 nm. The SEM analysis provided detailed information on the surface morphology, including the particle size, shape, and dispersion of Bi_2O_3 nanoparticles. The EDS analysis was employed to determine the chemical composition and identify the elements present in the nanocomposite structure, confirming the presence of bismuth (Bi), oxygen (O), carbon (C), and other constituent elements.

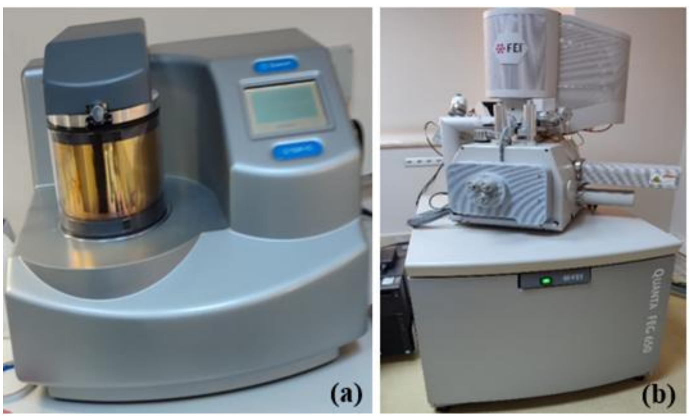

Figure 3. 4. Quorum brand thin film coating device (b) FEI brand SEM-EDS device.

3.2.2.2 Electromagnetic Shielding Tests

A review of the literature did not reveal prior studies on the electromagnetic shielding capability of Bi_2O_3 particles. This may be attributed to Bi_2O_3's low electrical conductivity compared to typical conductive materials used in shielding applications. Nonetheless, for a comprehensive characterization of the materials, electromagnetic shielding effectiveness (SE) tests were included in the project.

The SE tests were carried out in the Department of Electrical and Electronics Engineering at İskenderun Technical University. An Agilent N5234A PNA-L network analyzer, Maury X101A6 waveguide, and a Keysight X281A coaxial-to-waveguide adapter were used to perform the measurements in the 10 MHz – 43.5 GHz frequency range. The system was calibrated using a Keysight 85056A calibration kit prior to testing. The test setup and equipment are shown in Figure 3.5.

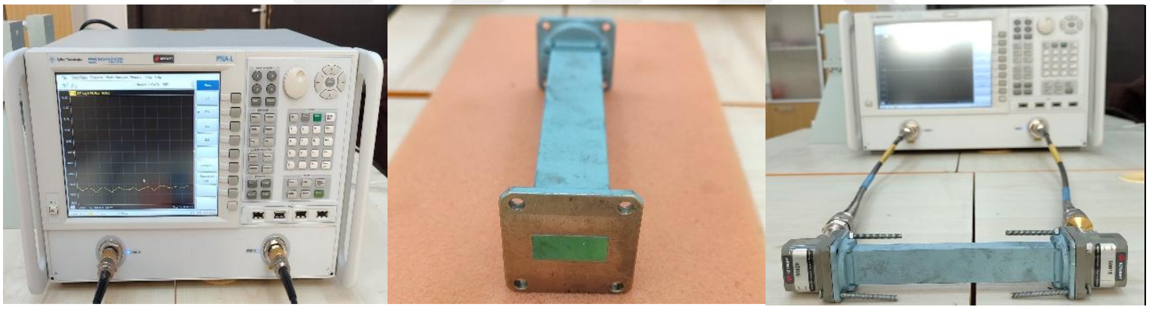

Figure 3. 5. Agilent N5234A PNA-L network analyzer and test setup.

Specimens were produced in thicknesses of 4, 7, and 10 mm, with input dimensions compatible with the waveguide aperture (10.16 mm × 22.86 mm). Transmission values (S12) were recorded with and without the samples in the 8–12 GHz X-band range at 1001 different frequency points. Shielding effectiveness in decibels (dB) was calculated for each sample using Equation 1, which relates the power of transmitted waves with and without the sample (Ozkan et al., 2020):

$$SE\ (dB) = 20\ \log_{10}\ (ET / Ei) \qquad \textbf{(Eq.1)}$$

Where ET is the transmitted wave with the specimen and Ei is the incident wave without the specimen.

3.2.2.3 Antibacterial Activity Tests

Antibacterial testing of the fabricated composite materials is critical to assessing their suitability for potential applications. One key area of use for radiation shields is in medical equipment and hospital environments, which inherently harbor diverse bacterial populations. Therefore, antibacterial performance testing was included in this project.

The tests were conducted in the microbiology laboratory of Chemvironbiotech, operating under the Çukurova University Technopark, according to the TS ISO 22196 standard, which is designed to measure antibacterial activity on plastics and other non-porous surfaces. The test bacteria used were S. aureus and E. coli strains. Test specimens were designed with dimensions of 5×5 cm as specified by the standard and were fabricated simultaneously with other test samples. Initially, the specimens were sterilized by immersion in 70% ethanol. Then, 0.4 mL of bacterial suspension was applied to the surface of each sample, and a 4×4 cm sterile film was placed on top of the inoculated area. Afterwards, the samples were placed in sterile Petri dishes and incubated at 35°C for 24 hours. Following incubation, the samples were transferred to Petri dishes containing Plate Count Agar (PCA) for bacterial growth assessment. The same procedures were applied to control samples without Bi_2O_3 reinforcement. The testing steps defined by the TS ISO 22196 standard are illustrated in Figure 3.6 (Microbe Investigations, 2023).

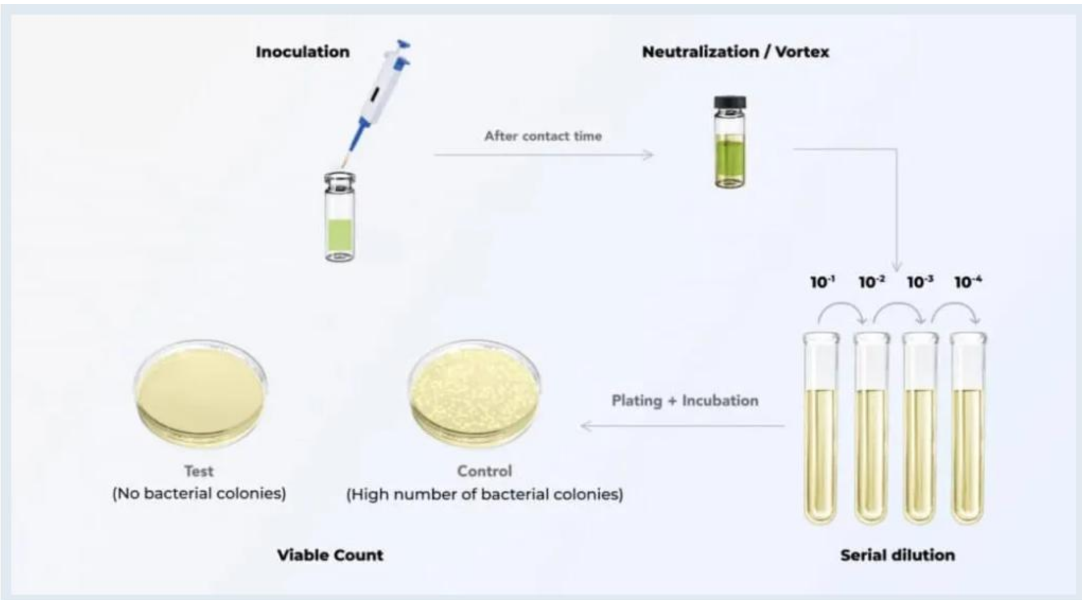

Figure 3. 6. Procedure Steps of the TS ISO 22196 Antibacterial Activity Test Standard.

3.2.2.4. Surface Resistivity Measurement

Surface resistivity measurements were conducted in accordance with the TS EN 1149-1 standard. This standard defines a method for determining surface resistance as an indicator of electrostatic discharge resistance. All measurements were performed under controlled environmental conditions at 25°C and 50% relative humidity. For each reinforcement ratio (1%, 3%, and 5%), measurements were repeated 5 times, and average values were recorded. A digital megohmmeter (ELME Multimeg) was used. Proper contact between the electrodes and the specimen was ensured during testing. Measurements were recorded in ohm/square. To ensure repeatability, electrodes were cleaned before each measurement and applied with consistent pressure. The samples were classified according to their resistivity (ohm/sq), as shown in Table 3.2 .

Table 3.2. Surface resistivity classification of materials (Ozkan, 2020)

Classification	Surface Resistivity (ohm/sq)
Conductive	$<10^{5}$
Dissipative	10^{5} to 10^{12}
Insulating	$>10^{12}$

4. RESULTS AND DISCUSSIONS

4.1. Morphological Structure Analysis

In this section, the structural changes in the surface morphology of Bi_2O_3 nanoparticle reinforced photopolymer composites at different additive ratios were investigated based on Scanning Electron Microscopy (SEM) and Energy Dispersive X-ray Spectroscopy (EDS) analysis results and discussed by comparing with literature findings. 200,000 times magnified SEM images taken from the produced samples are given in Figure 4.1. Also EDX analysis graphs are given in Figure 4.2.

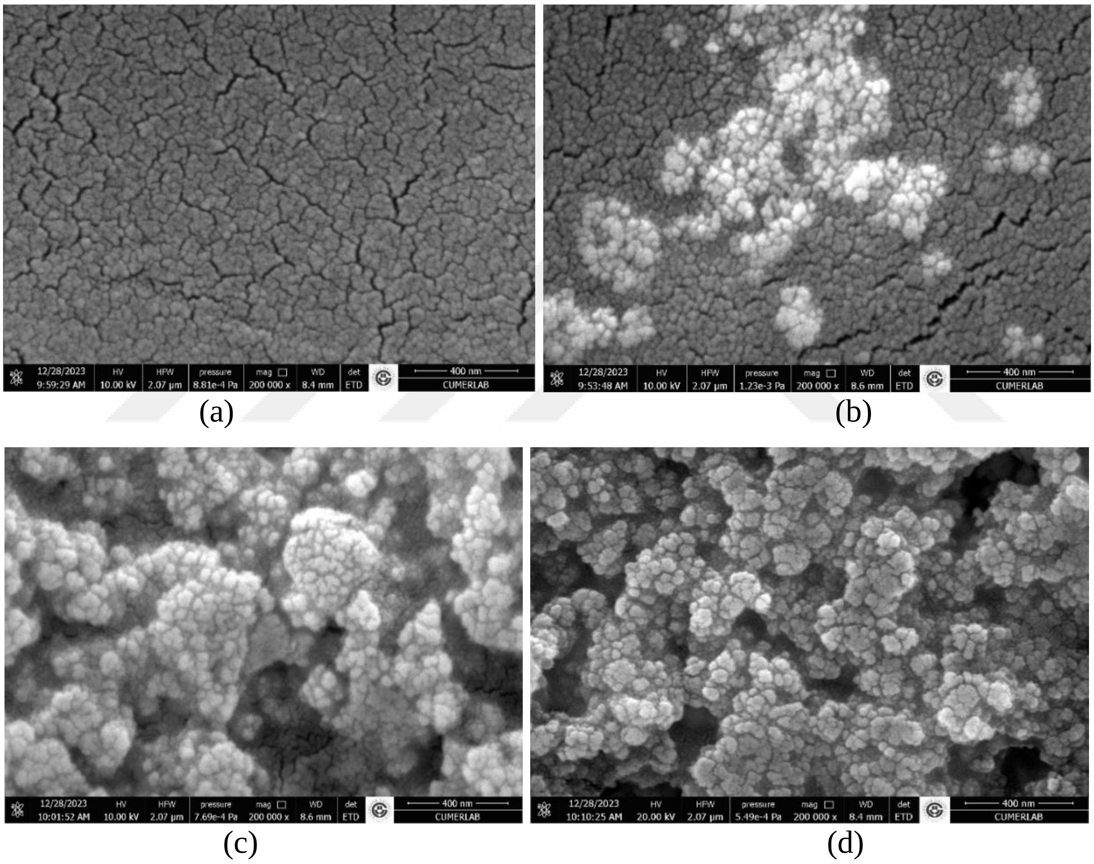

Figure 4. 1. SEM images magnified 200,000x; a) Undoped sample, b)1% doped, c)3% doped, d) 5% doped.

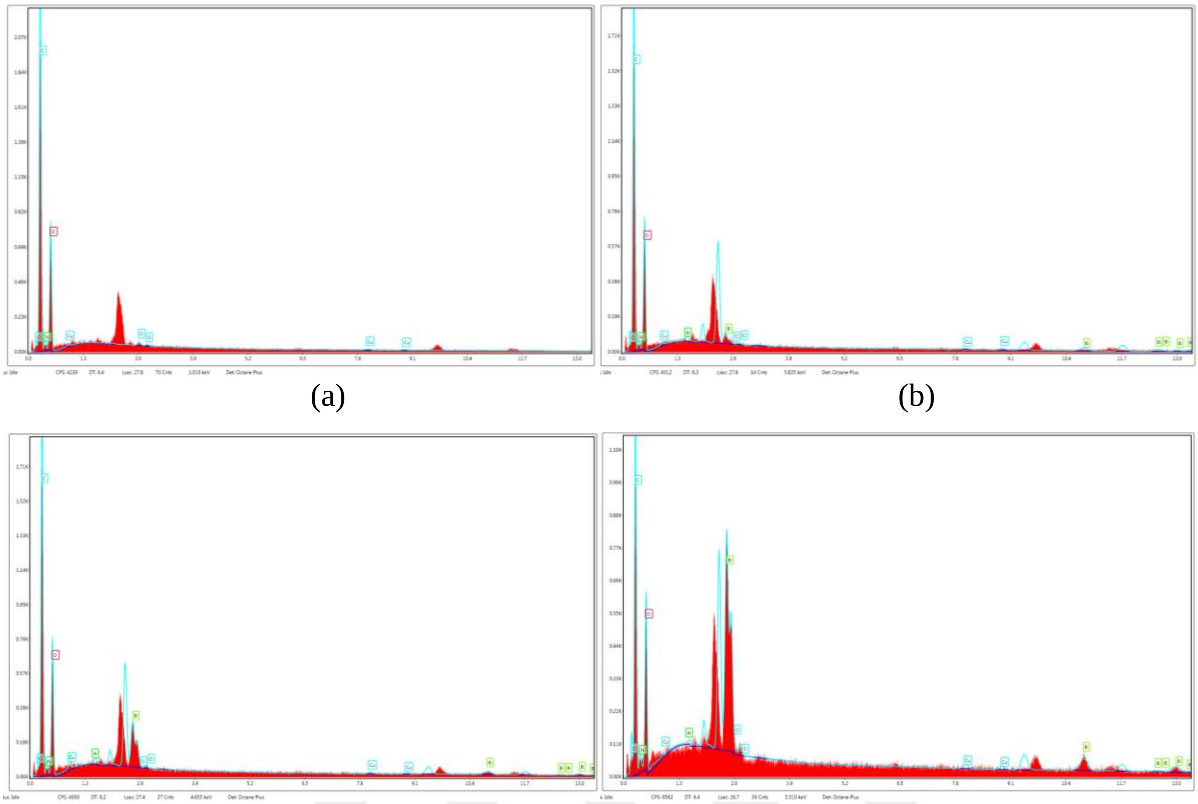

(a) (b)

(c) (d)

Figure 4. 2. EDX analysis graphs; a) Sample without additive, b) 1% additive, c) 3% additive, d) 5% additive.

It was observed that Bi_2O_3 nanoparticles were distributed quite homogeneously in the composite resin matrix at low doped rates. SEM examinations showed that there was no significant agglomeration on the surface of these samples and that the particles were regularly embedded in the resin matrix. Similarly, Alshahri et al. (2021) reported that low concentrations of Bi_2O_3 doped provided homogeneous distribution in LDPE-based systems and that the surface morphology was not deteriorated [29]. At medium doped rates (around 3%), micro-cluster formations were observed on the surface; however, it was determined that these clusters were limited and the general structure still maintained its homogeneity. Alruwaili and El Sayed (2024) stated that limited agglomerations started in the polymer matrix at similar filler rates and this led to an increase in surface roughness [30]. These local clustering regions on the surface were observed as brighter and denser areas in SEM images.

At high doping rates (>5%), significant agglomerations occurred. SEM images clearly show large nanoparticle clusters clustered together in some regions. Marshall et al. (2025) reported that similarly large agglomerations and heterogeneous structures were formed at Bi_2O_3 doping levels above 25%, and that these structures disrupted the surface morphology and negatively affected the composite performance [31]. In this study, it was determined that surface roughness and heterogeneity increased in samples with high doping rates. EDS analyses confirmed the presence of carbon, oxygen and bismuth elements in all samples. While the element distribution was more homogeneous at low doping rates, it was observed that bismuth concentrated in some regions at high doping rates. This situation coincides with the agglomeration regions observed with SEM and shows that nanoparticles are not distributed evenly in the matrix at high doping levels. Similarly, Ambika et al. (2017) reported that as the filling ratio increases, bismuth concentrates in certain regions in EDS maps and this reduces surface homogeneity [32]. EDX analyses give mass percentages of elements based on spectra taken from a certain surface area and therefore the results obtained reflect local concentrations in the analyzed region rather than the overall composition of the sample. When the EDX results used in this study were examined, it was observed that the Bi ratios detected increased significantly above the nominal values as the doping ratios increased. This difference is directly related to the characteristics of the SLA type 3D printer used in the production process. Comparative results are given in Table 4.1.

Table 4.1. Additive Percentages Detected in EDX According to Bi_2O_3 Additive Rates

Sample Code	**Nominal Bi_2O_3 Rate (%)**	**(%) Bi_2O_3 Rate Detected by EDX (%)**
Reference	0	0.00
1% additive	1	1.65
3% additive	3	6.96
5% additive	5	26.78

In SLA (Stereolithography) systems, the UV light source is located at the bottom of the printer and the layers are formed by curing with UV light applied to this sub-region of the photopolymer resin. The high-density Bi_2O_3 nanoparticles (approximately 8.9 g/cm^3) dispersed in the resin tend to settle to the lower layers under the influence of gravity during the production process. Therefore, even if the additive is homogeneously distributed in the sample, the particle density increases on the surfaces of the cured layers closest to the UV screen. If EDX analyses are performed from these depositional areas, the measured Bi percentage may be much higher than the nominal additive rate. For example, a very high Bi rate of 26.78% was detected in the 5% additive sample. This situation is not only due to agglomeration, but also to the concentration of particles on the surface that first comes into contact with the UV light. Similarly, the 6.96% Bi rate in the 3% additive sample can be evaluated as a result of sedimentation and local particle enrichment. In contrast, Bi element was not detected at all in the reference sample, confirming that there is no systematic error and that the Bi signal is only present in the doped samples. These findings reveal the difficulties in maintaining particle stability and dispersion throughout the production process in SLA-based photopolymerization systems and indicate the necessity of additional dispersion measures (e.g. viscosity increase, magnetic stirring, ultrasonic homogenization) for sedimentation control, especially in heavy metal oxide doped resins. As a result, as the Bi_2O_3 doping rate increased, visible changes occurred in the surface morphology; while a homogeneous and smooth surface structure was provided at low rates, surface integrity was impaired due to agglomeration and agglomeration at high rates. The fact that the doping rate should be carefully determined for optimum performance is supported by both the literature and the findings of this study.

4.2. Electromagnetic Shielding Effectiveness Test Results

Electromagnetic shielding effectiveness (EMSE) tests conducted on Bi_2O_3-filled polymer nanocomposites yielded limited shielding performance, as illustrated in Figure 4. 3.

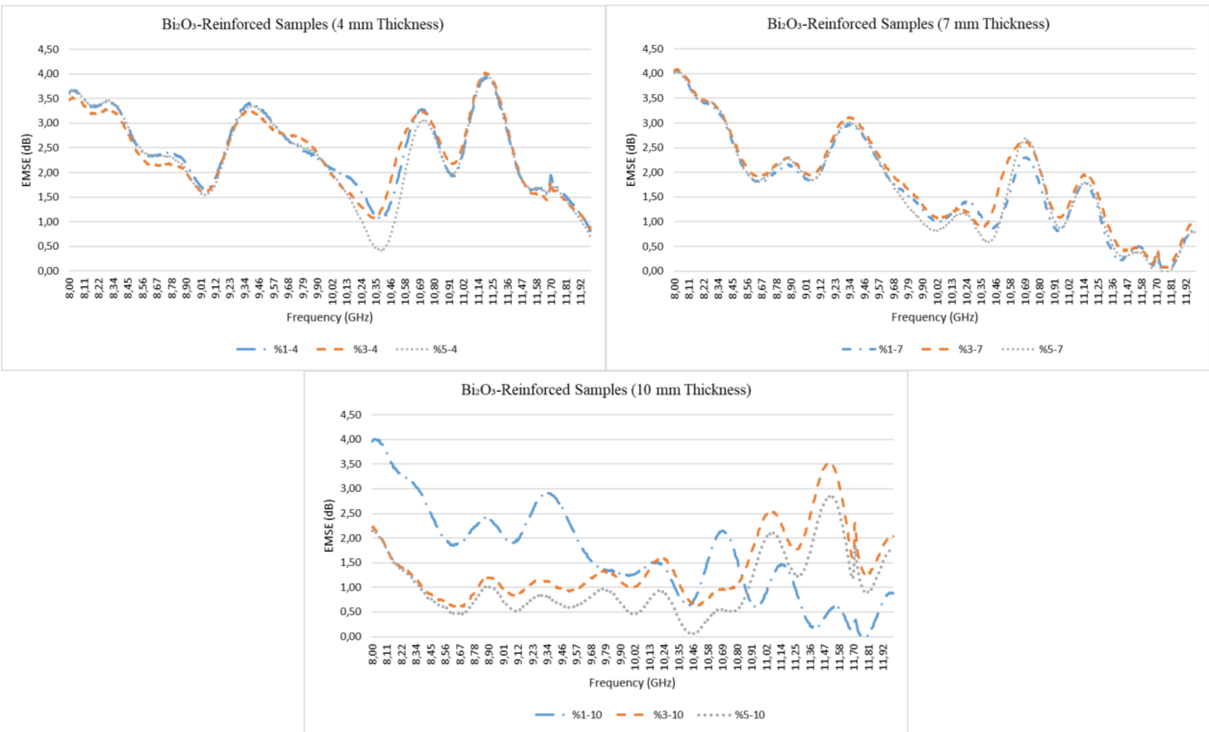

Figure 4. 3. EMSE Results of Bi_2O_3-Reinforced Samples.

As illustrated in Figure 1.11, electromagnetic shielding effectiveness (EMSE) values obtained from polymer composites containing 1, 3, and 5 wt.% Bi_2O_3 were consistently low across all tested sample thicknesses (4, 7, and 10 mm). Regardless of filler loading or thickness, the maximum EMSE did not exceed 5 dB in the 8–12 GHz frequency range. This clearly indicates that the Bi_2O_3 additive, in the absence of any conductive filler, contributes minimally to the attenuation of incident electromagnetic radiation.

This result aligns with previous findings in the literature. Bi_2O_3 is known to exhibit low electrical conductivity and primarily functions as a dielectric material with narrowband absorption (Liu & Yang, 2021; Maestre & Santos, 2023) [33,34]. The inability of Bi_2O_3 to form conductive networks significantly limits its shielding effectiveness, particularly in polymer matrices that also lack intrinsic conductivity. Maestre and Santos (2023) demonstrated that even at 5 wt.% Bi_2O_3 content in geopolymer composites, the improvement in EMSE was modest, increasing from 21.2 dB to only 23.6 dB [34]. This minor enhancement was attributed to better dispersion and interaction within a more structurally rigid matrix. In contrast, our polymer-based system, without synergistic fillers or conductive components, did not achieve such performance due to its lack of both conductivity and matrix rigidity. Liu and Yang (2021) also emphasized that effective shielding in their coating system was only achieved at high total filler contents (~45 wt.%) with optimized ratios of graphite, bismuth, and bismuth oxide [33]. At lower loadings or when Bi_2O_3 was used alone, EMSE remained weak. This underscores that Bi_2O_3 requires co-fillers with high electrical conductivity to contribute meaningfully to EMSE.

Comparatively, conductive filler-based systems outperform Bi_2O_3-dominant composites by a wide margin. For instance, Li et al. (2023) reported up to 113 dB of EMSE in PDMS matrices filled with 5 vol.% silver-coated fibers and 3 vol.% carbon nanotubes (CNTs) [35]. Similarly, Srivastava et al. (2017) achieved approximately 35 dB EMSE in polypyrrole/PVA films reinforced with silver nanoparticles [36]. Durmaz et al. (2023) showed that the addition of 10–30 wt.% carbon fiber to bio-based polymer matrices could raise EMSE to 28 dB in the X-band [37]. Even moderate levels of carbon-based fillers outperform Bi_2O_3. Rani et al. (2020) showed that incorporating 25 wt.% carbon black into PVA/PEG blends improved EMSE from 0.1 to 10.6 dB [38]. These results can be interpreted through percolation theory, which explains the rapid rise in shielding performance once a conductive network is established (Li et al., 2023) [35].

In conclusion, our findings confirm that the use of Bi_2O_3 alone does not offer meaningful electromagnetic shielding, even at higher loadings or increased thickness. Without the incorporation of conductive additives or the formation of a percolated structure, Bi_2O_3 remains functionally limited in EMI protection applications.

4.3. Antibacterial Efficacy of SLA-Printed Nanocomposite Surfaces

All Bi_2O_3-reinforced SLA nanocomposite surfaces containing 1 wt.%, 3 wt.%, and 5 wt.% Bi_2O_3 demonstrated strong antibacterial activity, consistently exceeding 99% bacterial reduction against E. coli and S. aureus after 24 h of contact in ISO 22196 tests. This level of efficacy is considered strongly antibacterial according to the standard (Pant et al., 2022) [39]. In our experimental results, the antibacterial activity was uniformly high across all tested loadings, indicating that even the lowest Bi_2O_3 concentration provided sufficient surface interaction to inactivate most bacteria.

Representative petri dish images (Figure 4. 4) display the colony formation immediately after bacterial inoculation (0 h) and the absence of colony growth after 24 h. The 0 h image shows dense colony distribution, while the 24 h image shows a complete absence of visible colonies, confirming a >99% reduction in viable cells. These visual outcomes validate the quantitative reduction observed in the ISO 22196 assays.

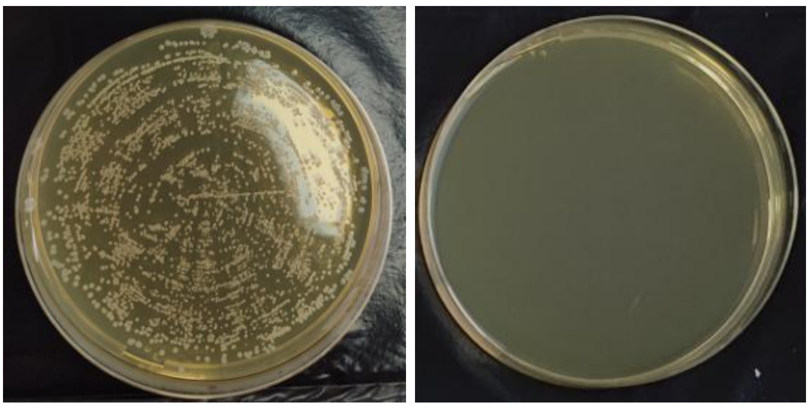

Figure 4. 4. Representative petri dish images showing bacterial colony formation at 0 h (left) and after 24 h (right) of contact with the Bi_2O_3-enhanced SLA surface.

Representative petri dish images showing bacterial colony formation at 0 h (left) and after 24 h (right) of contact with Bi_2O_3-reinforced SLA surface.

The high antibacterial performance of Bi_2O_3 is closely linked to its unique mechanism of action. Bismuth compounds primarily act by targeting bacterial metabolic pathways. Rather than relying on reactive oxygen species (ROS) generation or membrane rupture as seen in silver (Ag) and copper (Cu)-based systems, Bi_2O_3 interferes with key enzymatic activities, including those in the TCA cycle and oxidative phosphorylation. Liang et al. (2025) reported that bismuth disrupts bacterial respiration and energy production by inhibiting essential enzymes, eventually leading to cell death [40].

This metabolic inhibition mechanism has additional benefits: it is less likely to induce resistance development and poses lower toxicity risks to human cells compared to Ag and Cu. For instance, silver ions (Ag^+) are effective antimicrobials but tend to leach from surfaces, accumulate in tissues, and potentially cause cytotoxic effects (Ding et al., 2016; NIST, 2022)[41]. Copper also generates ROS and binds thiol-containing enzymes but may exhibit cytotoxicity if not carefully controlled (Grass et al., 2011; Liu et al., 2014) [42]. In contrast, Bi_2O_3 shows minimal ion release due to its low solubility, reducing the likelihood of adverse effects while still delivering potent antibacterial effects. Recent studies support our findings. Pant et al. (2022) demonstrated that α-Bi_2O_3 nanoparticles exhibited MIC values of 0.75 µg/mL against P. aeruginosa and 2.5 µg/mL against S. aureus [39]. Similarly, Parajuli et al. (2021) reported that Bi_2O_3 nanoflakes could fully suppress bacterial growth at concentrations as low as ~50 ppm [43]. These results align with our findings, where even the 1 wt.% Bi_2O_3 SLA composite completely suppressed colony formation after 24 h.

Overall, the ISO 22196-based results from our study confirm that Bi_2O_3 is a highly effective and safe antimicrobial additive for SLA-printed nanocomposites. The combination of strong antibacterial activity, stability, and biocompatibility makes Bi_2O_3 a promising candidate for applications requiring hygienic or biomedical surface properties.

4.4. Surfaces Resistivity Test Results

Surface resistivity measurements revealed that all SLA nanocomposites containing 1, 3, and 5 wt% Bi_2O_3 exhibited values exceeding $10^{12}\Omega$. This indicates an insulating behavior and the absence of an effective electronic conduction path within the composite structure. This insulating property directly limits the material's electromagnetic shielding effectiveness (EMSE). Since electromagnetic shielding relies heavily on mechanisms such as reflection and absorption (both of which are enhanced by sufficient electrical conductivity), the absence of a permeated conductive network hinders effective shielding [33,34]. In particular, reflection-based shielding is almost completely absent in insulating systems. Similar results have been reported in the literature. Maestre and Santos showed that geopolymer matrices filled with 5 wt% Bi_2O_3 exhibited limited conductivity and poor shielding performance, which was further deteriorated by agglomeration at higher filler concentrations. Wang et al. emphasized that it is not possible to create a permeation path without sufficient conductive filler loading, resulting in negligible protection values [44]. Similarly, Shukla reported that significant improvements in protection were achieved when conductive nanoparticles, such as iron-based fillers, were added to insulating polymer matrices [45]. Increasing the Bi_2O_3 ratio up to 5% did not provide significant SE values due to the absence of a conductive filler phase. These findings support the necessity of incorporating conductive fillers or using inherently conductive polymer systems when effective protection is desired in SLA-printed nanocomposites.

5. CONCLUSION

This thesis investigated the development of bismuth oxide (Bi_2O_3)-reinforced photopolymer nanocomposites fabricated via stereolithography (SLA) 3D printing and evaluated their performance in terms of antibacterial efficacy, electromagnetic shielding effectiveness (EMSE), and surface resistivity.

The composite samples were prepared with three different Bi_2O_3 loadings (1 wt%, 3 wt%, and 5 wt%) and coated onto cellulose-based nonwoven substrates. All samples were subjected to comprehensive characterization including visual inspection, surface conductivity tests, ISO 22196 antibacterial testing, and EMSE measurements within the X-band frequency range (8–12 GHz).

Surface resistivity measurements revealed that all Bi_2O_3-reinforced samples exhibited high values exceeding $10^{12}\Omega$, indicating strong electrical insulation properties. This finding was critical in understanding the subsequent EMSE results, which showed minimal shielding performance across all frequencies tested. The absence of a percolated conductive network in these formulations limited electromagnetic wave reflection and absorption capabilities, in line with the established literature that correlates EMSE with the presence of conductive pathways in composite materials.

In contrast, antibacterial test results were remarkably successful. According to TS ISO 22196 standard, all samples achieved >99% reduction in Staphylococcus aureus and Escherichia coli bacterial counts after 24 hours of surface contact. This performance confirms the inherent antimicrobial efficacy of Bi_2O_3, likely due to its ability to interfere with bacterial metabolic processes and cell structures, as supported by previous studies. Importantly, antibacterial activity was maintained across all loading levels, suggesting that even low filler concentrations are sufficient to impart strong biocidal effects in SLA-printed surfaces.

The visual evaluation of petri dish images before and after bacterial contact further supported these findings, demonstrating a sharp reduction in colony counts for all Bi_2O_3 formulations. These results suggest that while Bi_2O_3 is not effective as an electromagnetic shielding agent when used alone in non-conductive matrices, it provides a highly effective antibacterial surface in additive manufacturing applications.

In summary, this thesis concludes that Bi_2O_3-reinforced SLA nanocomposites are highly promising for antimicrobial applications where mechanical precision and biological safety are required. However, their use for EMI shielding is limited without additional conductive fillers or structural modifications aimed at enhancing charge transport properties. These findings provide a valuable foundation for future work in hybrid formulations and SLA-based functional surface coatings.

,

6. RECOMMENDATIONS

In light of the findings and limitations of this study, several directions are recommended for future research to expand the functionality and performance of SLA-printed Bi_2O_3-based nanocomposites. One of the most critical insights derived from the present work is the inherently low electromagnetic shielding effectiveness (EMSE) caused by the insulating nature of both Bi_2O_3 and the polymer matrix. To address this limitation, future investigations should consider the incorporation of conductive fillers such as carbon nanotubes, graphene, or silver nanoparticles alongside Bi_2O_3. Hybrid filler systems may enable the formation of conductive networks that allow for improved EM wave reflection and absorption while maintaining the antibacterial efficacy demonstrated in this study.

Furthermore, modifying the resin formulation itself may present new opportunities. Adjusting the SLA resin chemistry—through the introduction of functional monomers or tailored oligomers—could enhance filler dispersion and interfacial interactions, thus potentially improving electrical conductivity and electromagnetic performance. Additionally, taking full advantage of the SLA method's capacity for complex 3D geometries, future designs could incorporate structural engineering strategies such as layered or gradient filler distributions, conductive pathway architectures, or controlled porosity to enhance EM shielding even with low-conductivity materials.

Although antibacterial performance was highly successful, with over 99% reduction in E. coli and S. aureus across all filler concentrations, the long-term stability of this effect under varying environmental conditions such as humidity, UV exposure, and mechanical wear remains unexplored. Therefore, extended duration tests are necessary to verify the persistence of antimicrobial efficacy under realistic service conditions. In parallel, direct biocompatibility testing—such as cytotoxicity evaluations on mammalian cells—should be considered in order to assess the material's safety profile for biomedical applications. Lastly, to facilitate industrial translation, scale-up studies and cost-performance analyses are essential. The practicality of producing such nanocomposites on a commercial scale must be evaluated with consideration for print speed, resin cost, nanoparticle dispersion at bulk levels, and regulatory compliance. Moreover, future research could aim to develop multifunctional composites that go beyond antimicrobial and EM shielding performance by integrating mechanical durability, thermal resistance, and surface repellency.

REFERENCES

1. Sun, Q., Rizvi, G. M., Bellehumeur, C. T., & Gu, P. (2008). Effect of processing conditions on the bonding quality of FDM polymer filaments. Rapid prototyping journal, 14(2), 72-80. https://doi.org/10.1108/13552540810862028
2. Torrado, A. R., Shemelya, C. M., English, J. D., Lin, Y., Wicker, R. B., & Roberson, D. A. (2015). Characterizing the effect of additives to ABS on the mechanical property anisotropy of specimens fabricated by material extrusion 3D printing. Additive Manufacturing, 6, 16-29. https://doi.org/10.1016/j.addma.2015.02.001
3. Abourayana, H., Dobbyn, P., & Dowling, D. (2018). Enhancing the mechanical performance of additive manufactured polymer components using atmospheric plasma pre-treatments. Plasma Processes and Polymers, 15(3), 1700141. https://doi.org/10.1002/ppap.201700141
4. Torrado, A. R., & Roberson, D. A. (2016). Failure analysis and anisotropy evaluation of 3D-printed tensile test specimens of different geometries and print raster patterns. Journal of Failure Analysis and Prevention, 16, 154-164. https://doi.org/10.1007/s11668-016-0067-4
5. Gardner, J. M. et al. (2016). 3-D printing of multifunctional carbon nanotube yarn reinforced components. Additive Manufacturing, 12, 38-44. https://doi.org/10.1016/j.addma.2016.06.008
6. Gkartzou, E., Koumoulos, E. P., & Charitidis, C. A. (2017). Production and 3D printing processing of bio-based thermoplastic filament. Manufacturing Review, 4, 1. https://doi.org/10.1051/mfreview/2016020
7. Podsiadły, B., Matuszewski, P., Skalski, A., & Słoma, M. (2021). Carbon nanotube-based composite filaments for 3d printing of structural and conductive elements. Applied Sciences, 11(3), 1272. https://doi.org/10.3390/app11031272
8. Fico, D., Rizzo, D., Casciaro, R., & Esposito Corcione, C. (2022). A review of polymer-based materials for fused filament fabrication (FFF): focus on sustainability and recycled materials. Polymers, 14(3), 465. Https://doi.org/10.3390/polym14030465
9. Shah, M. et al. (2023). The Influence of Nanoparticle Dispersions on Mechanical and Thermal Properties of Polymer Nanocomposites Using SLA 3D Printing. Crystals, 13(2), 285. https://doi.org/10.3390/cryst13020285
10. Aumnate, C., Pongwisuthiruchte, A., Pattananuwat, P., & Potiyaraj, P. (2018). Fabrication of ABS/graphene oxide composite filament for fused filament fabrication (FFF) 3D printing. Advances in Materials Science and engineering, 2018, 1-9. https://doi.org/10.1155/2018/2830437
11. V-Niño, E. D., Lonne, Q., Díaz Lantada, A., Mejía-Ospino, E., Estupiñán Durán, H. A., Cabanzo Hernández, R., ... & Endrino, J. L. (2020). Physical and chemical properties characterization of 3d-printed substrates loaded with copper-nickel nanowires. Polymers, 12(11), 2680. https://doi.org/10.3390/polym12112680
12. Aktitiz, İ., Varol, R., Akkurt, N., & Saraç, M. F. (2020). In-situ synthesis of 3D printable mono-and Bi-metallic (Cu/Ag) nanoparticles embedded polymeric structures with

enhanced electromechanical properties. Polymer Testing, 90, 106724. https://doi.org/10.1016/j.polymertesting.2020.106724
13. Chiulan, I., Voicu, Ş. I., & Batalu, D. (2022). The use of graphene and its Derivatives for the development of polymer matrix composites by stereolithographic 3D printing. Applied Sciences, 12(7), 3521. https://doi.org/10.3390/app12073521
14. Shinde, V. V., Celestine, A. D., Beckingham, L. E., & Beckingham, B. S. (2020). Stereolithography 3D printing of microcapsule catalyst-based self-healing composites. ACS Applied Polymer Materials, 2(11), 5048-5057. https://doi.org/10.1021/acsapm.0c00872
15. Singh, B., Kumar, R., & Chohan, J. S. (2020). Polymer matrix composites in 3D printing: A state of art review. Materials Today: Proceedings, 33, 1562-1567. https://doi.org/10.1016/j.matpr.2020.04.335
16. FDM vs SLA: FDM ve SLA Farkı Nedir? (2020, February 27). 3D3 Teknoloji. https://3d3teknoloji.com/blog/fdm-vs-sla-fdm-ve-sla-farki-nedir/#:~:text=SLA%20yani%20Stereolithography%203D%20yaz%C4%B1c%C4%B1, Son erişim tarihi: 13.08.2025
17. https://store.anycubic.com/products/photon-m3-max, Son erişim tarihi: 13.08.2025
18. Eren, O., Nurullah Yüksel, & İsmail Şahin. (2024). Investigation of mechanical and electrical properties of photopolymer nanocomposites reinforced with carbon-based nanoparticles produced by digital light processing 3D printing technique. Polymer Composites. https://doi.org/10.1002/pc.29271
19. Qiu, S., Li, S., Tao, Y., Feng, X., Yu, B., Mu, X., … Jie, G. (2015). Preparation of UV-curable functionalized phosphazene-containing nanotube/polyurethane acrylate nanocomposite coatings with enhanced thermal and mechanical properties. *RSC Advances*, *5*(90), 73775–73782. https://doi.org/10.1039/c5ra12264c
20. Chiara Ingrosso, Carola Esposito Corcione, Raffaella Striani, Comparelli, R., Marinella Striccoli, Agostiano, A., … Mariaenrica Frigione. (2015). UV-Curable Nanocomposite Based on Methacrylic-Siloxane Resin and Surface-Modified TiO2 Nanocrystals. ACS Applied Materials & Interfaces, 7(28), 15494–15505. https://doi.org/10.1021/acsami.5b03731
21. Abatay, E. (2015). Development of antibacterial polymer-based nanocomposite materials, Master's thesis, İzmir Institute of Technology, Graduate School of Engineering and Sciences. İzmir, Turkey.
22. Amrhar, R., Singh, J., Eesaee, M., Carrière, P., Saidi, A., & Nguyen-Tri, P. (2025). tablePolymeric Nanocomposites-based Advanced Coatings for Antimicrobial and Antiviral Applications: A Comprehensive Overview. Results in Surfaces and Interfaces, 100497. https://doi.org/10.1016/j.rsurfi.2025.100497
23. Díez-Pascual, A. M., & Luceño-Sánchez, J. A. (2021). Antibacterial Activity of Polymer Nanocomposites Incorporating Graphene and Its Derivatives: A State of Art. Polymers, 13(13), 2105. https://doi.org/10.3390/polym13132105
24. Olmos, D., & González-Benito, J. (2021). Polymeric Materials with Antibacterial Activity: A Review. *Polymers*, *13*(4), 613. https://doi.org/10.3390/polym13040613

25. Avila, M. A., Bonilla-Cruz, J., Méndez-Nonell, J., & Lara-Ceniceros, T. E. (2020). Enhanced mechanical and thermal properties of SLA 3D printed structures by incorporating controllably annealed anatase TiO_2 nanoparticles. Materials Research Express, 7(11), 115316. https://doi.org/10.1088/2053-1591/abc8cf
26. Gil, L. D., Monteiro, S. N., & Colorado, H. A. (2024). Polymer matrix nanocomposites fabricated with copper nanoparticles and photopolymer resin via vat photopolymerization additive manufacturing. Polymers, 16(17), 2434. https://doi.org/10.3390/polym16172434
27. Adefuye, O. A., Raji, N. A., Adedeji, K. A., Fadipe, O. L., & Olowu, B. (2019). ADDITIVE MANUFACTURING AND SAND-CASTING FOUNDRIES PRACTICES IN NIGERIA. *Engineering and Technology Research Journal*, *4*(1), 55–63. https://doi.org/10.47545/etrj.2019.4.1.049
28. Anycubic Photon M3 Max. (2025). Retrieved August 27, 2025, from Anycubic Wiki website: https://wiki.anycubic.com/en/resin-3d-printer/photon-m3-max
29. Alshahri, S., Alsuhybani, M., Alosime, E., Almurayshid, M., Alrwais, A., & Alotaibi, S. (2021). LDPE/Bismuth Oxide Nanocomposite: Preparation, Characterization and Application in X-ray Shielding. Polymers, 13(18), 3081. https://doi.org/10.3390/polym13183081
30. Alruwaili, A., & El Sayed, A. M. (2024). Characterization and the physical properties of nano-sized Bi2O3/polymer for energy and high-refractive index applications. Results in Physics, 61, 107746. https://doi.org/10.1016/j.rinp.2024.107746
31. Marshall, S. K., Boonpeng, K., Buapud, N., Chimhashat, S., Chuaymuang, J., Kwandee, P., & Songphum, N. (2025). Bismuth Oxide Nanoparticle-Enhanced Poly(methyl methacrylate) Composites for I-131 Radiation Shielding: A Combined Simulation and Experimental Investigation. Polymers, 17(5), 590. https://doi.org/10.3390/polym17050590
32. Ambika, M. R., Nagaiah, N., Harish, V., Lokanath, N. K., Sridhar, M. A., Renukappa, N. M., & Suman, S. K. (2017). Preparation and characterisation of Isophthalic-Bi2O3 polymer composite gamma radiation shields. Radiation Physics and Chemistry, 130, 351–358. https://doi.org/10.1016/j.radphyschem.2016.09.022
33. Liu, Y. J., & Yang, Y. F. (2021). Textile Research Journal, 91(17–18), 1986–1998. https://doi.org/10.1177/0040517521994342
34. Maestre, C. V., & Santos, G. N. (2023). Effect of bismuth oxide nanoparticle on the electromagnetic interference shielding and thermal stability of industrial waste based-geopolymer composites. Scientific Reports, 13(1). https://doi.org/10.1038/s41598-023-27623-2
35. Li, J., Sun, H., Yi, S.-Q., Zou, K.-K., Zhang, D., Zhong, G.-J., … Li, Z.-M. (2022). Flexible Polydimethylsiloxane Composite with Multi-Scale Conductive Network for Ultra-Strong Electromagnetic Interference Protection. Nano-Micro Letters, 15(1). https://doi.org/10.1007/s40820-022-00990-7
36. Srivastava, J., Kumar Khanna, P., V More, P., & Singh, N. (2016). Chemically Synthesized Ag/PPy-PVA Polymer Nanocomposite Films As Potential EMI Shielding

Material In X-band. Advanced Materials Letters, 08(01), 42–48. https://doi.org/10.5185/amlett.2017.6486

37. Bedriye Ucpinar Durmaz, Salman, A. O., & Ayse Aytac. (2023). Electromagnetic Interference Shielding Performances of Carbon-Fiber-Reinforced PA11/PLA Composites in the X-Band Frequency Range. ACS Omega, 8(25). https://doi.org/10.1021/acsomega.3c01656
38. Rani, P., Ahamed, M. B., & Deshmukh, K. A. (2020). Materials Research Express, 7(6), 065001. https://doi.org/10.1088/2053-1591/ab9853
39. Pant, B. D., Benin, B. M., Nalin Abeydeera, Kim, M.-H., & Huang, S. D. (2022). Bi2O3 nanoparticles exhibit potent broad-spectrum antimicrobial activity and the ability to overcome Ag-, ciprofloxacin- and meropenem-resistance in P. aeruginosa: the next silver bullet of metal antimicrobials?. Biomaterials Science, 10(6), 1523–1531. https://doi.org/10.1039/d1bm01844b
40. Rosário, S., Fábio Mosso Moreira, Albina, L., Guerra, W., & Priscila Pereira Silva-Caldeira. (2023). Biological Activities of Bismuth Compounds: An Overview of the New Findings and the Old Challenges Not Yet Overcome. Molecules, 28(15), 5921–5921. https://doi.org/10.3390/molecules28155921
41. NIST Standard Reference Materials® 2022 Catalog NIST SP 260-176. (2022). Retrieved from https://tsapps.nist.gov/publication/get_pdf.cfm?pub_id=934102
42. Mikolay, A., Huggett, S., Tikana, L., Grass, G., Braun, J., & Nies, D. H. (2010). Survival of bacteria on metallic copper surfaces in a hospital trial. Applied Microbiology and Biotechnology, 87(5), 1875–1879. https://doi.org/10.1007/s00253-010-2640-1 Zhong, L., Wang, L., Xu, L., Liu, Q., Jiang, L., Zhi, Y., … Zhou, P. (2014). The role of NOS-mediated ROS accumulation in an early phase Cu-induced acute cytotoxicity in MCF-7 cells. BioMetals, 28(1), 113–122. https://doi.org/10.1007/s10534-014-9807-7
43. Geoffrion, L. D., Medina-Cruz, D., Kusper, M., Sakr Elsaidi, Watanabe, F., Prakash Parajuli, … Grégory Guisbiers. (2021). Bi2O3 nano-flakes as a cost-effective antibacterial agent. Nanoscale Advances, 3(14), 4106–4118. https://doi.org/10.1039/d0na00910e
44. Nan, X., Zhang, Y., Shen, J., Liang, R., Wang, J., Jia, L., … Zhang, Z. (2024). A Review of the Establishment of Effective Conductive Pathways of Conductive Polymer Composites and Advances in Electromagnetic Shielding. Polymers, 16(17), 2539–2539. https://doi.org/10.3390/polym16172539
45. Shukla, V. (2019). Review of electromagneticinterference shielding materials fabricated by iron ingredients. NanoscaleAdvances, 1(5), 1640–1671. https://doi.org/10.1039/C9NA00108E